A novel method for preparing microcrystalline films from the amorphous phase by shot-like IR laser light irradiation

メタデータ	言語: English 出版者: 公開日: 2008-02-14 キーワード (Ja): キーワード (En): 作成者: KONDO, S, SAITO, T メールアドレス: 所属:
URL	http://hdl.handle.net/10098/1616

A novel method for preparing microcrystalline films from the amorphous phase by shot-like IR laser light irradiation

S. Kondo and **T. Saito**

Research Center for Development of Far-Infrared Region, Fukui University, Bunkyo,
Fukui 910-8507, Japan

PACS 61.80.Ba, 78.55.Hx, 78.66.Nk, 81.15.Ef, 81.40.Tv

A novel method is presented for preparing microcrystalline films of metal halide semiconductors. The method is based on fast crystallization and subsequent crystal growth of amorphous films by means of shot-like IR laser light irradiation and includes *in situ* monitoring of exciton luminescence. It is possible to prepare high-quality microcrystalline films at various size levels of the crystallites. There is an optimum size level at which the microcrystalline films show much stronger free-exciton luminescence than polycrystalline films and bulk single crystals (as exemplified for CuCl and $CsPbCl_3$). The microcrystalline films provide extremely densely dispersed nanoparticles for studying mesoscopic enhancement of linear and nonlinear optical properties at various particle size levels.

1 Introduction

Nanodimensional particles of semiconductors have attracted much attention over the last two decades or more owing to mesoscopic enhancement of linear and nonlinear optical properties. Various efforts have been made to obtain nanodimensional particles according to the object of investigation. In studies of the quantum size effect on excitons, the particles are usually embedded in transparent bulk materials (crystals or glasses). Such specimens have mostly been prepared by means of quenching of the thermal equilibrium for phase separation of a eutectic mixture. The resulting nanoparticles necessarily have a size distribution reflecting the phase equilibrium. Furthermore, the mole fraction of the particles is generally very small, typically of the order of 0.1 mol% or less. Preparation of specimens containing nanoparticles of a definite size with a high concentration is not only desirable for basic research of mesoscopic properties but also for studies of the applications.

Many metal halide semiconductors such as silver (e.g. [1]), thallium (e.g. [2]), copper (e.g. [3]), lead (e.g. [4]), and cadmium (e.g. [5]) halides, including their mixed systems [6], can be rendered amorphous by quench deposition, yielding film samples. The amorphous films exhibit excellent transmittance below the absorption edge and have a well-defined, characteristic crystallization temperature at which their absorption spectra drastically change in outline (e.g. see the inset of Fig. 1). The films, when crystallized just above the crystallization temperature, are generally in a microcrystalline state, and change into a polycrystalline state when they are subsequently annealed at higher temperatures. Many of the crystalline films produced via the amorphous phase, whether they are microcrystalline or polycrystalline in nature, show very high transmittance compared with polycrystalline films directly deposited onto hot substrates. It is expected that the microcrystalline films can provide extremely densely dispersed nanoparticles of high quality for studying mesoscopic enhancement of optical properties.

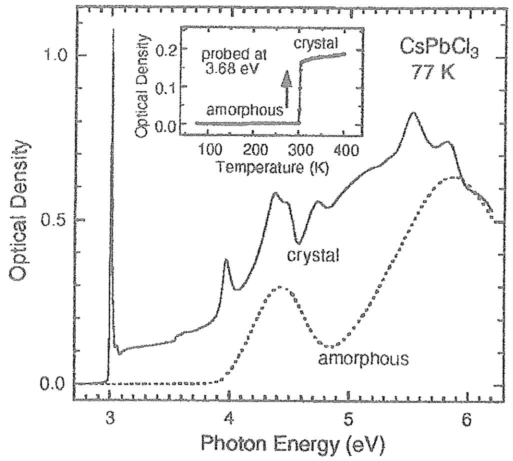

Fig. 1 Absorption spectra of CsPbCl$_3$ films at 77 K for the amorphous (dashed curve) and crystalline (solid curve) states. The inset shows the change in optical density during slow heating (1 K/min), revealing that the crystallization temperature is 302 K.

In the present work we report the development of a novel method for preparing microcrystalline films of metal halides at various microcrystallite size levels from the amorphous phase. The method is based on shot-like IR laser light irradiation and involves *in situ* exciton spectroscopy of the films. The method has been successfully applied to several metal halides (CuX, TlX, CsPbX$_3$ (X = Cl, Br), the optical properties of which are characterized by sharp exciton resonance). In the present paper we briefly describe the method and present a few results to show the potential usefulness of the method.

2 Experimental

It is well known that exciton spectroscopy provides a powerful means for investigating the crystallinity of materials on a nanometric scale when the materials show sharp exciton resonance (e.g. [7]). Therefore, exciton spectroscopy is frequently used for characterizing nanoparticles or quantum dots (e.g. [8]). In particular, the full width at half maximum (FWHM) and peak energy of free-exciton emission bands can be used to judge the quality, size, and size distribution (e.g. [9]); also, emission due to trapped excitons (if any) gives a measure for the 'bad quality' (e.g. [10]). In our method for producing microcrystalline films of metal halides from the amorphous phase, the experimental setup is designed to exploit these advantages of exciton spectroscopy for the purpose of *in situ* monitoring of the formation and subsequent growth of nanodimesional crystals in the films.

Figure 2 shows a schematic view of the experimental setup. It allows for the preparation of amorphous films and then transformation of the films into various (nano-, micro-, and poly-) crystalline states with simultaneous monitoring of the transformation process using *in situ* exciton spectroscopy. The films are

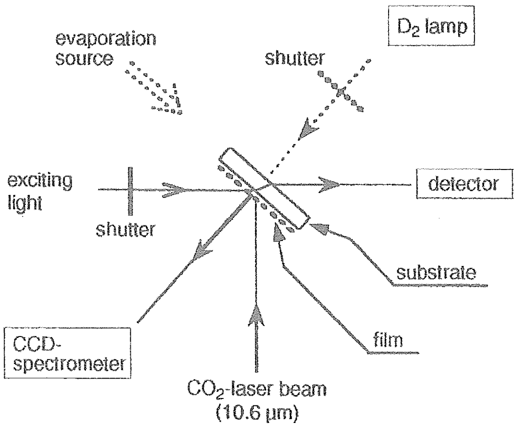

Fig. 2 Schematic view of the experimental setup.

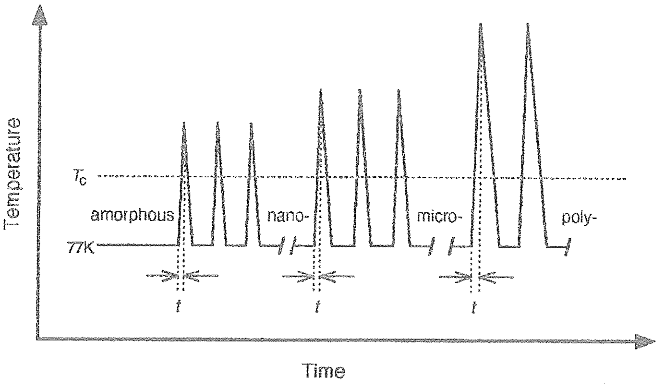

Fig. 3 Rapid cycles of heating to above the crystallization temperature, T_c, and cooling to 77 K, performed on amorphous films to yield, in a stepwise fashion, crystallites of various sizes. The heating times, *t*, are in the range 10–1000 ms. The current state of the films is monitored by intermittently, but synchronously, measuring photoluminescence and absorption spectra (at 77 K).

located at the center of the vacuum chamber of a cryostat. The substrate for the films is vertically attached to the top of the cold finger of the cryostat and the cold finger can be rotated on the vertical axis. The vacuum chamber has four silica-glass and one ZnSe windows (whose centers lie on the same horizontal plane) for optical measurements and IR laser light irradiation, respectively. In the evaporation source unit, a tungsten basket heating element, placed 8 cm from the center of the vacuum chamber (and, thus, from the substrate), is employed to vaporize the source material of the films in a controlled manner, and a rotatable shutter is used to cut off the vapor flow as required.

We prepared amorphous films of various metal halides by quench deposition of the vapor flow of the compounds onto silica-glass substrates cooled to 77 K in a vacuum of about 9×10^{-6} Pa. The films were then subjected to rapid cycles of heating to above the crystallization temperature, T_c, and cooling to 77 K in a manner illustrated by Fig. 3, in order to achieve, in a stepwise fashion, various mean sizes of crystalline products in the films. This was performed by means of shot-like IR laser light irradiation of the films using a continuous-wave CO_2 laser (wavelength, 10.6 μm; power, 10 W), with the cold finger of the cryostat being held at 77 K. The spot size of the CO_2 laser beam (Gaussian beam) was set to be about 3 mm in diameter at the film position using ZnSe lens optics. One shot caused one cycle of rapid heating/cooling. The irradiation time (*t* in Fig. 3) per shot was in the range 10–1000 ms, depending on the desired crystallite sizes.

To monitor the current state of the films during the repeated heating/cooling cycles, photoluminescence and absorption spectra of the films were intermittently, but synchronously, measured (at 77 K) using a liquid nitrogen-cooled CCD spectrometer equipped with a 0.47 m grating monochromator, using fiber optics as a light guide for the emitted light. Real-time displays of the spectra were obtained using trigger pulses in a synchronous manner. A 500 W xenon lamp in combination with a 0.5 m grating monochromator was used as the light source for the measurement of luminescence spectra, and a 30 W deuterium lamp was employed to measure absorption spectra. The emissions irradiating the films were focused at the center of the CO_2 laser-crystallized spot of the films, with an irradiation area of about 0.8×0.8 mm^2 for the luminescence measurements and about 0.6 mm in diameter for the absorption measurements. In the following discussion the CO_2 laser-crystallized micro- or polycrystalline spots in the films will be referred to as micro- or polycrystalline films.

3 Results

We will briefly describe typical results for CuCl ($T_c = 177$ K [11]), whose quantum size effects on excitons have been extensively studied for microcrystals dispersed in bulk matrices but not for microcrystal-

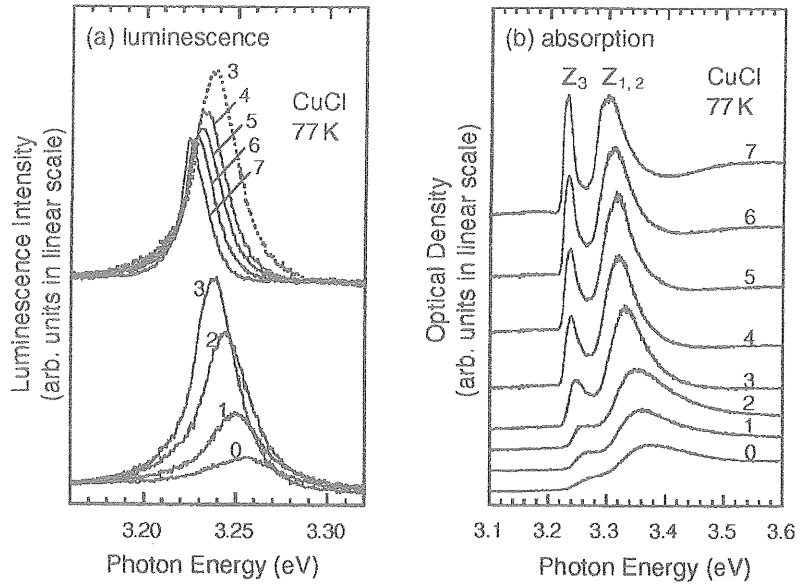

Fig. 4 Sequential change of (a) the luminescence and (b) the absorption spectra of a CuCl film (95 nm thick) corresponding to the rapid heating/cooling cycles illustrated in Fig. 2. The spectra are differently shifted along the y-axis for clarity. The luminescence was excited at 3.54 eV.

line films, and for $CsPbCl_3$ (T_c = 302 K [12]), which is known to be one of the most luminescent semiconductors [13].

Figure 4b shows the sequential changes of the absorption spectra measured in the Z_3 and $Z_{1,2}$ exciton absorption region and Fig. 4a shows photoluminescence spectra excited at 3.54 eV (350 nm), the sample for both figures being a CuCl film (95 nm thick). The numbers 0–7 in Fig. 4 indicate the extent of the heat treatment to which the film was subjected: the larger the number (heat treatment number, HTN), the more heavily heat-treated the film by the repetition of the heating/cooling operation. The HTN for the as-deposited film was denoted '0'. (As reported in [11], exciton absorption is possible even in the amorphous state, because of the very small radius and very large binding energy of the excitons, e.g. 0.7 nm and 213 meV, respectively, for the Z_3 excitons.) With an increase of the HTN, both the absorption and the luminescence spectra shift to lower energies. Although the absorption intensity monotonically increases with HTN, the luminescence has a maximum intensity for a HTN of 3, after which the luminescence intensity decreases with increasing HTN. We note that for both the absorption and luminescence measurements, the spectral profile (peak energies, peak intensities, and FWHM) for a HTN of 7 was unchanged on further repetition of the heating/cooling cycles with the longest heating duration of 1000 ms.

Similar results are obtained for $CsPbCl_3$, as shown in Fig. 5. In this case exciton absorption is missing in the amorphous state (see Fig. 1), in contrast to the case of CuCl. Crystalline proportions are 0.24 and 0.40 for HTNs of 1 and 2, respectively, and 1 for larger HTNs, which are the ratios of the integrated absorption intensities for the respective HTNs to that for the highest HTN, 7, in the photon energy region up to 3.9 eV (note that in this region the amorphous portion in the film is transparent, see Fig. 1). The spectra for the highest HTN are characterized by the strongest exciton absorption peak and the weakest emission peak. The strongest luminescence intensity, normalized with respect to the crystalline proportions, is exhibited for a HTN of 3 (the luminescence spectra in Fig. 5a are not normalized).

We heat-treated several amorphous films with thickness in the range 80–150 nm for both compounds (CuCl and $CsPbCl_3$). In all the films, a maximum in the integrated (normalized) luminescence intensity was observed at particular, intermediate steps of the heat treatment. The peak energies of the emission bands with the maximum integrated intensity were almost the same for all the films, showing values of

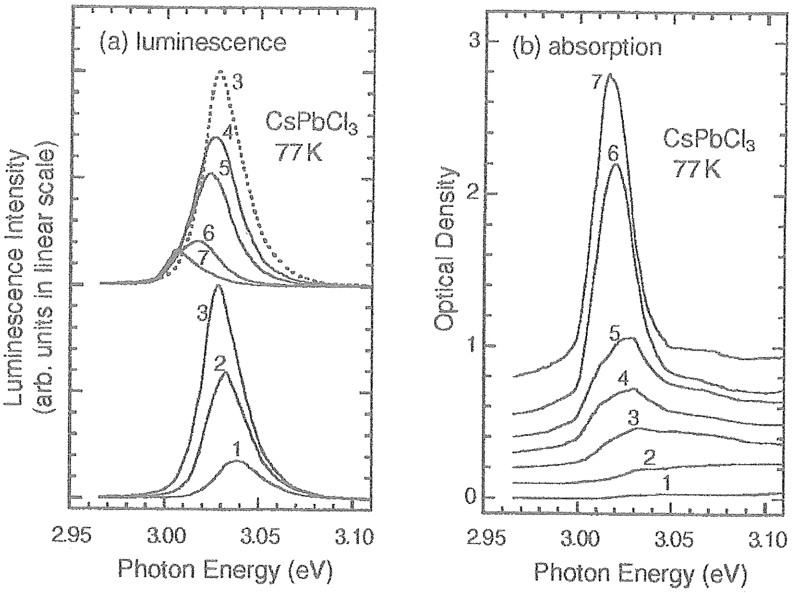

Fig. 5 Sequential change of (a) the luminescence and (b) the absorption spectra of a $CsPbCl_3$ film (150 nm thick). The luminescence was excited at 3.26 eV.

3.240 eV for CuCl and about 3.027 eV for $CsPbCl_3$, which were blue-shifted with respect to the peak energies of the emission bands for the highest HTN in the compounds by 15 and about 19 meV, respectively. The ratio of the maximum integrated intensity to the integrated intensity of the emission band for the highest HTN varied from film to film, but was always in the range 2.5–4 for CuCl and 5–20 for $CsPbCl_3$.

4 Discussion

For CuCl (Fig. 4), all the luminescence spectra have their peak energies at the peak positions of the corresponding Z_3 exciton absorption, indicating that the luminescence is due to the Z_3 free-exciton emission. The peak energy (3.225 eV) and FWHM (14 meV) of the luminescence spectrum for a HTN of 7 are almost the same as those of the Z_3 free-exciton emission band (at 80 K) reported for polycrystalline CuCl films [14] grown on (0001) Al_2O_3 substrates and preferentially oriented along the ⟨111⟩ direction. (In [14], luminescence spectra measured as a function of temperature for a film of 100 nm thickness are presented in the temperature range 10–70 K with a spacing of 10 K, whose extrapolation yields a peak energy of about 3.225 eV and FWHM of about 13 meV at 80 K for the Z_3 free-exciton band.) Strain effects on the CuCl film, and thus on the CuCl exciton energy, thermally induced by the substrate are not considerable, since such effects have been ruled out for CuCl films with a thickness larger than 10 nm [15]. In what follows the films heavily heat-treated up to the highest HTN are referred to as the polycrystalline films, although the sizes of the "polycrystallites" were not measured. With a decrease of HTN, the peak energies of the Z_3 free-exciton emission bands shift to higher energies. The blue shift of the peak energy demonstrates the effect of quantum confinement on the Z_3 free excitons – grain boundaries in the microcrystalline state provide confinement barriers for the excitons, whereas in the amorphous state the excitons are confined within a size defined by the short-range order, which increases with increasing temperature below T_c [11]. We note that a trace of the I_1 bound-exciton emission due to a neural acceptor (Cu^+ vacancy [16]) was by no means detected for all HTNs (in [14], the same trace is evidently detected at 3.20 eV at 70 K). All the luminescence spectra are only composed of single, Z_3 free-exciton bands without exhibiting any other emission band, suggesting a high-quality nature of the film. It is noted that excitons even in the microcrystalline film are free from being trapped, despite the expectation [17] of a high density of surface states. The line broadening of the free-exciton emission band with decreasing HTN is considered to be due to a size distribution of the crystallites in the film.

The largest blue shift, 30 meV, which is observed for a HTN of 0, corresponds to an effective radius for the exciton confinement (EREC) of 2.3 nm, if we assume the effective-mass approximation in the weak confinement regime [18] using the Z_3 free-exciton mass, $2.3m_0$ (where m_0 is the electron mass). The blue shift, 15 meV, of the emission band with the maximum integrated intensity corresponds to an EREC of 3.3 nm. This value (3.3 nm) may be taken as an optimum crystallite size at which the free-exciton luminescence efficiency of the CuCl films is maximized.

It is notable that the free-exciton luminescence efficiency for CuCl is strongly enhanced, by a factor of 2.5–4, for the microcrystalline state with the optimum EREC, 3.3 nm, as compared to that for the polycrystalline state. There are two possibilities for the physical origin of the enhanced luminescence. One is the occurrence of new radiative decay processes resulting from ballistic collisions of the free excitons at the *boundaries of the microcrystallites*, a microcrystalline counterpart of so-called wall collisions (ballistic collisions at the *film surfaces*). The other is concerned with the giant oscillator strength effect characteristic of excitonic superradiance. The quantum yield of the free-exciton emission in the microcrystalline CuCl films with the optimum microcrystallite size is expected to be very high compared to that in bulk CuCl, because even polycrystalline films exhibit stronger free-exciton luminescence than bulk single crystals due to wall collisions [15].

Concerning $CsPbCl_3$, whose luminescence properties were reported for amorphous and microcrystalline films in a previous paper [19], the mean crystallite size for the polycrystalline state (the highest HTN of 7 in Fig. 5) is 25 nm in diameter (which was determined by an X-ray diffraction method) as compared with the exciton radius of 1 nm. The luminescence spectra in the crystalline phase are due to free-exciton emission. The blue shift, about 19 meV, of the emission band with the maximum integrated intensity corresponds to an effective microcrystallite diameter of 4.1 nm, which was determined simply by comparing the blue shift with the reported blue shift versus diameter [20] (in [20], the diameter versus blue shift is given for $CsPbCl_3$ microcrystals embedded in CsCl crystals). The free-exciton luminescence efficiency for $CsPbCl_3$ is greatly enhanced, by a factor of 5–20, for the microcrystalline state with the optimum effective microcrystallite diameter, 4.1 nm, as compared to that for the polycrystalline state; the latter state is, however, still characterized by stronger free-exciton luminescence than single crystals. The physical origin of the enhancement is related to the occurrence of excitonic superradiance [19]. We note that, under high-density excitation, the microcrystalline state showed superradiance-enhanced strong stimulated emission suggesting a very short gain length, in contrast to the case of the polycrystalline state and of bulk single crystals. In bulk single crystals, stimulated emission has been observed only for a particular, long-optical-path geometry of high-density excitation [21]. Details are reported elsewhere [22].

5 Conclusion

We have developed a novel method for preparing microcrystalline films of metal halide semiconductors by means of shot-like IR laser light irradiation of amorphous films using a continuous-wave CO_2 laser. The formation of nanodimensional crystals and their subsequent growth in the films can be monitored using *in situ* exciton absorption/luminescence spectroscopy. It is possible to obtain high-quality microcrystalline films at various size levels of the crystallites.

The method has been successfully applied to several metal halide semiconductors. The potential of the method has been shown by discussing a few results for CuCl and $CsPbCl_3$. There is an optimum mean microcrystallite size (3.3 nm radius for CuCl and 4.1 nm diameter for $CsPbCl_3$) at which the films exhibit, in their heat treatment history, the strongest free-exciton luminescence with a much higher (by a factor of 2.5–4 for CuCl and 5–20 for $CsPbCl_3$) quantum yield than that of their polycrystalline state, but with the polycrystalline state still exhibiting a strong free-exciton emission band as compared to that for bulk single crystals. To our knowledge, the results provide the first straightforward demonstration of confinement-induced enhancement (mesoscopic enhancement) of free-exciton luminescence using the same starting specimens, i.e. the same quantities, or numbers, of molecules – such a direct comparison of the quantum yield for microcrystals with that for polycrystals (or bulk crystals) is difficult to carry out for microcrystals dispersed in bulk matrices because of thermal decomposition/generation of the molecules during heat treatments [7]. It is evident that the present method can be used as an alternative means to prepare specimens for studying mesoscopic enhancement of linear and nonlinear optical properties of metal halide nano- or microcrystals at various size levels.

References

[1] H. G. Gottwald, T. Lieser, K. G. Weil, and A. Weiss, Z. Naturforsch. A **40**, 677 (1985).
[2] S. Kondo, T. Itoh, S. Saito, and M. Mekata, Solid State Commun. **78**, 557 (1991).
[3] H. G. Gottwald and K. G. Weil, Ber. Bunsenges. Phys. Chem. **92**, 60 (1988).
[4] S. Kondo, H. Maruyama, and T. Saito, phys. stat. sol. (a) **147**, 453 (1995).
[5] S. Kondo, S. Kagawa, and T. Saito, phys. stat. sol. (b) **154**, 583 (1996).
[6] S. Kondo, K. Amaya, and T. Saito, J. Phys.: Condens. Matter **15**, 971 (2003).
[7] M. Haselhoff and H.-J. Weber, Phys. Rev. **58**, 5052 (1998).
[8] S. V. Gaponenko, Optical Properties of Semiconductor Nanocrystals (Cambridge University Press, 1998), pp. 84–152.
[9] J.-S. Lee, in: Semiconductor Quantum Dots – Physics, Spectroscopy and Applications, edited by Y. Masumoto and T. Takagahara (Springer Verlag, Berlin/Heidelberg/New York, 2002), pp. 1–57.
[10] B. D. Yao, Y. F. Chan, and N. Wang, Appl. Phys. Lett. **81**, 753 (2002).
[11] S. Kondo and T. Seki, Mater. Sci. Eng. B **15**, 133 (1992).
[12] S. Kondo, T. Sakai, H. Tanaka, and T. Saito, Phys. Rev. B **58**, 11401 (1998).
[13] L. N. Amitin, A. T. Anistratov, and A. I. Kuznetsov, Sov. Phys. Solid State **21**, 2041 (1979).
[14] M. Nakayama, H. Ichida, and H. Nishimura, J. Phys.: Condens. Matter **11**, 7653 (1999).
[15] M. Nakayama, A. Soumura, K. Hanasaki, H. Takeuchi, and H. Nishimura, Phys. Rev. B **55**, 10099 (1997).
[16] C. Weeker and S. Nikitine, J. Phys. Chem. Solids **30**, 2135 (1969).
[17] F. Henneberger and J. Puls, Optics of Semiconductor Nanostructures, edited by F. Hennenberger, S. Schmitt-Rink, and E. Göbel (Akademie Verlag, Berlin, 1993), pp. 497–543.
[18] T. Itoh, Y. Iwabuchi, and M. Kataoka, phys. stat. sol. (b) **145**, 567 (1988).
[19] S. Kondo, H. Nakagawa, T. Saito, and H. Asada, J. Phys.: Condens. Matter **14**, 1247 (2003).
[20] M. Nikl, K. Nitsch, K. Polak, E. Mihokova, S. Zazubovich, G. P. Pazzi, P. Fabeni, L. Salvini, R. Aceves, M. Barbosa-Flores, R. Perez Salas, M. Gurioli, and A. Scacco, J. Lumin. **72–74**, 377 (1997).
[21] I. Baltog, L. Mihut, and S. Lefrant, J. Lumin. **68**, 271 (1996).
[22] S. Kondo, K. Suzuki, T. Saito, H. Asada, and H. Nakagawa, Phys. Rev. B **70**, 205322 (2004).